

OXYGEN BINDING AND ACTIVATION WITH HEMOPROTEINS: MODEL APPROACH USING
IRON-PORPHYRIN COMPLEXES

Zen-ichi Yoshida

Department of Synthetic Chemistry,
Kyoto University, Yoshida, Kyoto 606, Japan

Abstract — Using myoglobin reconstituted with synthetic hemes, the structure-oxygen binding relationship is investigated. Oxygen affinity is controlled by (1) the basicity of heme iron and (2) site specific interaction of the peripheral substituents of heme with globin side chain. The effect of hydrophobic cavity size on the oxygen binding is examined by using the hydrocarbon chain-bridged metalloporphyrin-imidazole complexes (metal: Fe(II), Co(II)). The stability of oxy form of this model complexes changes with the fitness of the cavity. As oxygenase, L-tryptophan pyrrolase is taken up. Fe(II)porphyrin is shown to be the best model of its active site. This model complex effectively catalyzes the oxygenation of 3-substituted indoles to form products corresponding to formylkynurenine (the oxygenation product of L-tryptophan) with 40-50% conversion of the substrate. ESR analysis of the oxygenation system indicates cooperative electron transfer (COET) occurs from the substituted indole anion to the oxygen in the ternary system: indole anion \cdots Fe(II)porphyrin \cdots O₂. This type of electron transfer is a new concept that should occur in any strong donor \cdots Fe(II)porphyrin \cdots acceptor system. The COET process for L \cdots Fe(II)porphyrin \cdots O₂ complex is discussed with the ionization potential value of L as a criterion.

INTRODUCTION

Hemoproteins play a very important role in maintaining the life of all vertebrates. The active site of hemoproteins is known to be heme (iron porphyrin complex), although they exhibit the different biological function such as (1) reversible oxygen binding for transport and storage (hemoglobin and myoglobin), (2) oxygenation with molecular oxygen (mono-oxygenase: eg. cytochrome P-450, and dioxygenase: eg. L-tryptophan pyrrolase), (3) oxygen reduction (cytochrome c oxidase), (4) electron transfer (cytochrome b and c) and (5) hydrogen peroxide utilization (catalase and peroxidase). We discuss the structure-function relationship in myoglobin and L-tryptophan pyrrolase using the model of their active site, because they have the same heme (protoheme). The most significant problem in both cases is why the protoheme of their active site can stabilize or activate molecular oxygen.

1. REVERSIBLE OXYGEN BINDING

Of the respiratory proteins (Ref. 1⁴), myoglobin (Mb) is a monomer, whereas hemoglobin (Hb) is a tetramer ($\alpha_2\beta_2$) composed of two similar globins of unequal length. Although their aminoacid sequences are different than each other, all Mb and Hb globin-heme units consisting of eight helical regions (A^H). The proximal histidine for Mb and Hb is always the eighth residue in helical region F (F8 His). The protoheme of Hb and Mb is wedged in a crevice between segments E and F as shown in Fig. 1. Oxygen binds on the E (distal) side surrounded by the hydrophobic peptide sidechain. The protoheme in Hb and Mb is considered to regulate the oxygen affinity and to provide the kinetic stabilization to the iron-dioxygen group. For example the existence of the hydrophobic pocket and the proximal histidine (imidazole) coordination to the heme iron(II) should be important for favorable formation of the reversible Mb-O₂ (or Hb-O₂) complex. On the other hand, electronic and steric effects of peripheral substituents as well as electronic state of the heme iron should influence on the oxygen affinity of Hb and Mb. However these problems are still vague. In this section, the oxygen affinity of monomer in the homoproteins is discussed by using (1) reconstituted Mb and (2) bridged porphyrin ("handbag porphyrin")-iron complexes. This is because of elimination of the cooperative effect owing to the interaction between the monomer proteins from the observed oxygen affinity.

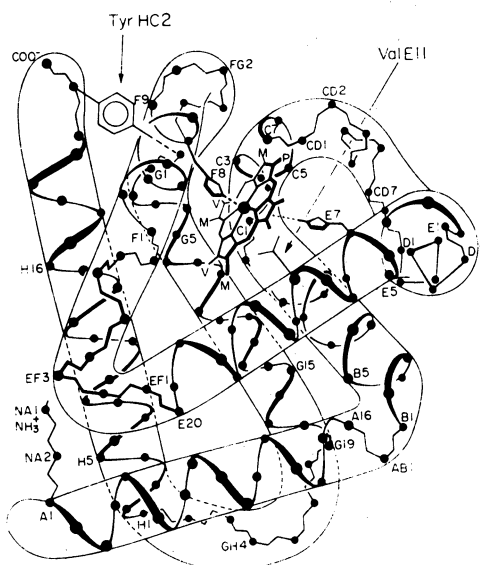
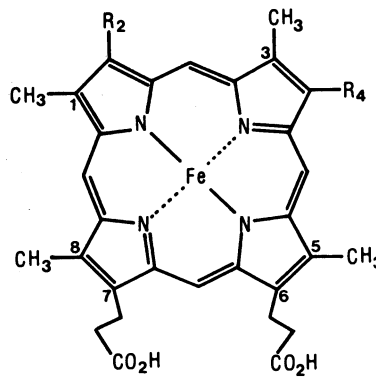


Fig. 1 Structure of monomer (β -chain) in Hb (Perutz, Ref. 1)

1.1 Oxygen binding of reconstituted Mb

We have synthesized various porphyrins and prepared their hemins (see Table 1) by incorporation of iron to the porphyrin dimethyl ester followed by its hydrolysis with 20% HCl. Recombination of these hemins with sperm whale apo-Mb has been carried out according to the known procedure (Ref. 5) to get the reconstituted met Mb (r-met Mb). In order to elucidate the electronic effect of the peripheral substituents toward the heme iron, the pKa value of the H_2O -coordinated met Mb has been determined (Ref. 5, 6) at 25°C. The result is shown in Table 1. The pKa value shown in this table is considered to be a measure of basicity (relative electron density) of the heme iron (even for heme iron (II)). After reduction of the r-met Mb to the corresponding reconstituted Mb (r-Mb) by enzymatic reduction system (Ref. 5), oxygen binding equilibrium was investigated using the automatic recording method of Imai et al. (Ref. 7). In each case, the Hill coefficient is nearly unity, indicating no cooperative interaction between the proteins of r-Mb. The value of oxygen pressure at half saturation, P_{50} (measure for oxygen affinity) is summarized in Table 1. Since the heme iron(II)- O_2 interaction is primarily controlled by the donor property of the heme-iron(II), the increase of electron donating power of the peripheral substituents (i.e. pKa value) is



Heme used

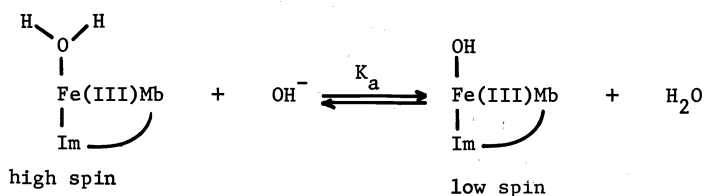


Table 1 Oxygen Affinity (P_{50} at pH 7.0, 25°C) and pKa (25°C) of Reconstituted Sperm Whale Mb

Heme	R ₂	R ₄	P ₅₀	pKa
Proto (nat)	CH=CH ₂	CH=CH ₂	0.93	8.95 (a)
Proto (rec)	CH=CH ₂	CH=CH ₂	0.91	
Deutero	H	H	0.33	9.10 (b)
Meso	C ₂ H ₅	C ₂ H ₅	0.66	(9.4) (b)
2-Et-Deutero	C ₂ H ₅	H	0.40	9.32
DIP	i-Pr	i-Pr	3.98	9.68
Pempto	H	CH=CH ₂	0.68	8.91

(a) Antonini et al (1971), (b) La Mar et al (1978)

considered to enhance the oxygen affinity. This is a case for Deutero-Mb. However as is seen in Table 1, the oxygen affinity of DIP-Mb is smallest among the r-Mb inspite of its largest pKa value. This is attributed to the site specific steric effect between the isopropyl group at 2-position of the heme and the residue (Me₂CHCH₂CH<) of E 15 leucin in the E segment (see Fig. 2).

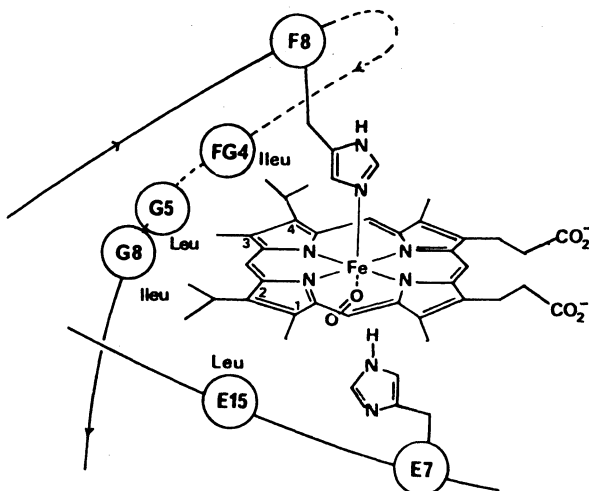


Fig. 2 Oxygen binding structure around the heme of Mb

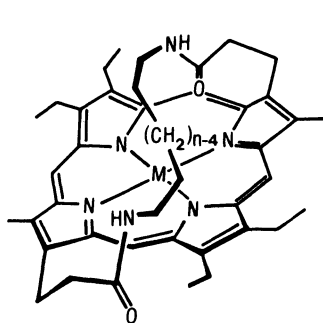
By this steric interaction, the distance between the E segment and the heme is increased (i.e. the hydrophobic pocket becomes large) with the bulkiness of R₂ group, resulting in the decrease of oxygen affinity by weakening the interaction of distal imidazole (N) with bound O₂. The X-ray data of Mb (Ref. 8) suggest that the R₂ group of heme is placed in the position where the steric interaction with the E 15 leucine residue (and E 11 valine residue) is very easy to occur (example to be compared: Mb and Pempto-Mb). The R₄ group of heme is also possible to interact spacially with the CD 1 phenylalanine residue from the distal side to distort the heme plane (Ref. 3). This distortion should decrease the interaction of bound O₂ with the distal imidazole (example to be compared: Meso-Mb and 2-Et-Deutero-Mb). Also the rate of autoxidation (r-Mb·Fe(II)O₂ + H⁺ → r-Mb·Fe(III)OOH) of the oxy form of r-Mb with proton as well as the data shown in Table 2 suggest that the size of the hydrophobic pocket regulates the stability of the r-Mb·Fe(II)O₂.

1.2 Oxygen binding with bridged metalloporphyrins

In order to examine the effect of hydrophobic cavity size on the stability of $r\text{-Mb}\cdot\text{Fe(II)}\text{O}_2$, we have synthesized the [n]-hydrocarbon chain-bridged porphyrins and prepared their iron and cobalt complexes (I) (Ref. 9). The stability of the oxyform of the bridged iron(II)-porphyrin ($n=6\sim 14$) in the following solvent-reducing agent systems is determined by spectroscopic method: solvent system I: CH_2Cl_2 -N-ethylimidazole/phosphate buffer (pH 7) with sodium dithionite

solvent system II: Toluene-N-ethylimidazole with NaBH_4

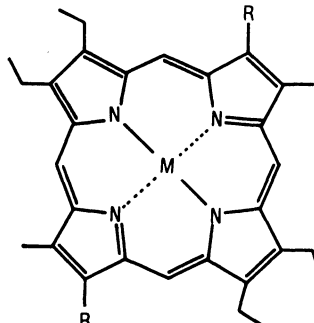
solvent system III: DMF-N-ethylimidazole with NaBH_4



I

[n]-Bridged Metalloporphyrin

M: Fe, Co, n: 6 ~ 14



II

Reference Metalloporphyrin

R: $\text{CH}_2\text{CH}_2\text{CONHR}'$ (R': n-propyl or n-hexyl)

The observed half life time of the oxy form in each solvent system at 233°K and 273°K is summarized in Table 2. The stability of [n]-hydrocarbon chain-bridged iron(II) porphyrin·(N-ethylimidazole)· O_2 is clearly shown to become large with decreasing cavity size until $n=6$. The CPK model for the oxygen adduct indicates that the bound oxygen best fits for the cavity of the [6] bridged one.

Table 2 Half Life Time (min) of [n]-Hydrocarbon Chain-Bridged Iron(II)porphyrin·(N-Ethylimidazole)· O_2

Solvent system	233°K			273°K		
	I	II	III	I	II	III
n=6	*1	110	170	*1	8	15
8	-	70	160	-	5	15
10	-	60	100	-	5	14
12	-	60	110	-	5	13
14	-	60	110	-	5	13
ref. *2	-	45	55	-	0.5	1.5

*1) very short. *2) reference compound II

Other than the cavity size, temperature and character of the solvent system also greatly affect to the stability of "oxy form" as shown in Table 2. For example, the half life time of all oxygen adduct examined ($n: 6\sim 14$ and reference compound) is so short that the spectra of oxygen adduct is not observed even at low temperature (-30°C). Table 2 suggests that the stability of oxygen adduct much depends on the polarity of solvent and presence of proton. Dipolar aprotic solvent stabilizes the oxygen adduct, on the other hand the oxygen adduct is rapidly oxidized in the presence of proton. This behavior is consistent to that of oxy Mb as described above. Although it is not able to obtain the oxy form of the bridged heme (I, M: Fe(II)) at room temperature, the [n]-bridged Co(II)porphyrin (I, M: Co(II), n: 7, 10, 12, 14) is found to form the reversible oxygen binding adduct at ambient temperature (eg. 25°C). For example, the reversible oxygen binding with [12] bridged Co(II)porphyrin in DMF-benzimidazole is illustrated in Fig. 3. The absorption spectra

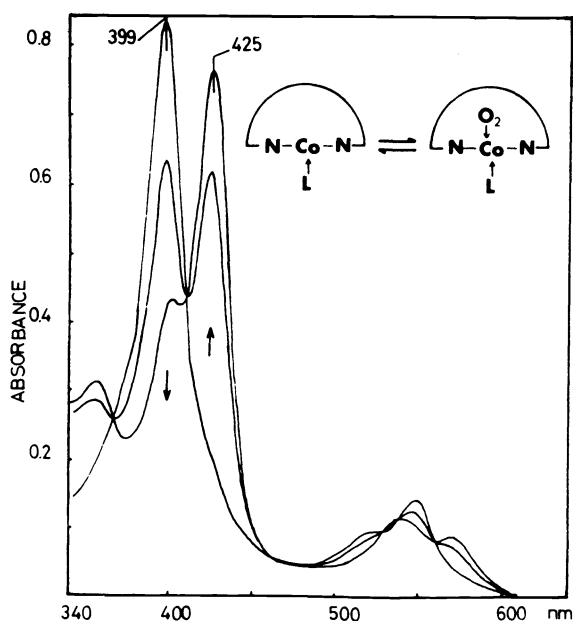


Fig. 3 Absorption spectra of reversible oxygenation of [12] bridged Co(II)porphyrin in DMF-benzimidazole (L), 25°C

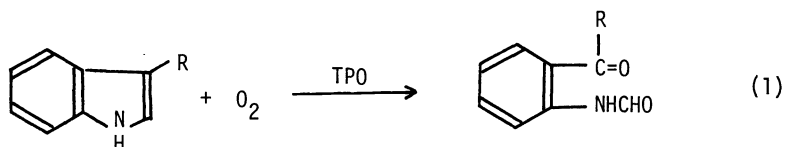
(399, 550 nm) observed in the absence of oxygen are a typical pattern of the deoxyform (the five coordinated monoamin adduct). On the other hand, the absorption spectra (425, 540, 565 nm) observed in the presence of oxygen indicate the formation of the 1:1 stoichiometric complex, [12] bridged Co(II)porphyrin·(benzimidazole)·O₂. N-ethylimidazole behaves similar to benzimidazole. It is to note that the rate of incorporation of oxygen greatly depends on hydrophobic chain length. The shorter the chain length is, the slower the oxygen absorption. Thus [14] or [12] bridged Co(II)porphyrin absorbs the molecular oxygen faster than the other bridged Co(II)porphyrins (n: 7, 10) and even the reference compound (II, M: Co(II), R': n-hexyl). The ESR parameters and characteristics of the deoxy and oxy [n] bridged Co(II)porphyrin·N-ethylimidazole complexes are very similar to those of CoMb and CoHb. It is important to point out that imidazole nitrogen (>N) is very significant for the formation of reversible oxygen adduct (Im-Fe(II)P-O₂) in the bridged metalloporphyrin as well as in the reconstituted Mb.

2. OXYGEN ACTIVATION IN OXYGENASE SYSTEMS

Since independent discovery of the oxygenases a large number of papers concerning oxygenases have been reported (Ref. 2, 10~14). However, oxygen activation mechanisms in the oxygenase system still remains obscure. We discuss the oxygen activation in tryptophan pyrrolase (TPO) based on our experimental results using iron-porphyrin complexes as the model for the active site of this enzyme.

2.1 Tryptophan pyrrolase model reaction and activation of oxygen

TPO catalyses the reaction of tryptophan (R: CH₂CH(NH₂)CO₂H) with molecular oxygen to form formylkynurenine (FK) according to reaction 1.



The most remarkable feature of this enzyme reaction system (Ref. 2) is that the presence of a reductase system is not required. Detailed analysis of the TPO reaction indicates that the reduced TPO (Fe(II)TPO) is the active form of this enzyme and that TPO has two kinds of binding sites which form the substrate-enzyme adduct (EFe²⁺·S₁S₂) with tryptophan. This adduct's interaction with molecular oxygen yields the oxygenated adduct (EFe²⁺·S₁S₂·O₂), which decomposes to FK and EFe²⁺·S₁ (see Figure 4). As shown in Table 3, the electronic spectra of Fe(II)TPO, Fe(III)TPO, and Fe(II)TPO·O₂ are very similar to those of myoglobin (Ref. 15, 16). As mentioned in Section 1, the heme in myoglobin is considered to be surrounded by the hydrophobic peptide side chain (Fig. 1). Based on the spectral similarity

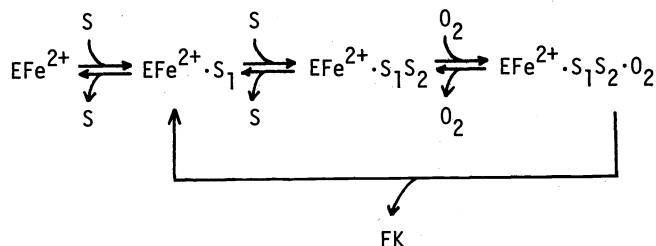


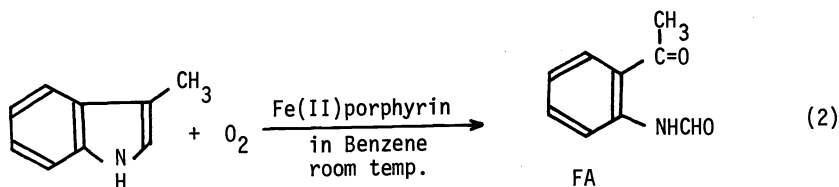
Fig. 4 TPO reaction cycle

Table 3 Absorption Maximum of Fe(II)TPO, Fe(III)TPO, Fe(II)TPO·TRY·O₂ and Those of the Corresponding Myoglobin (nm)

	Oxidized Form			Reduced Form		Oxygenated Form		
Tryptophan Pyrrolase	405	502	632	433	555	418	545	580
Myoglobin (Sperm whale)	409	505	635	434	556	418	543	581

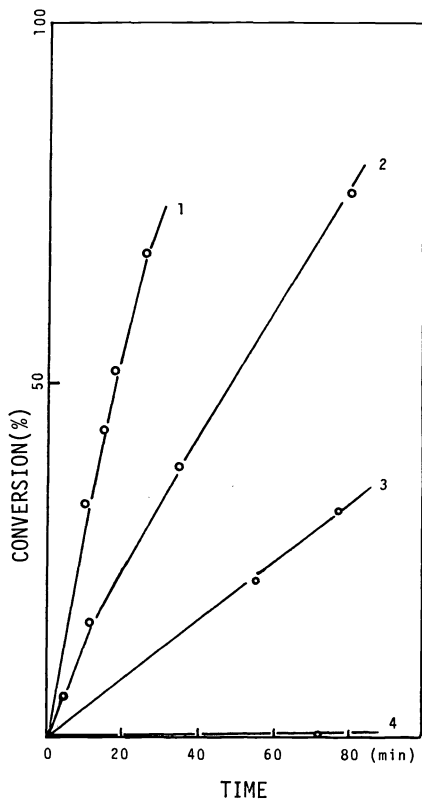
between myoglobin and TPO, we deduced that the surrounding structure of the heme in TPO is similar to that in myoglobin. For designing the enzyme model, it is important to consider the functional and structural similarity between the model and the active site of enzyme. With this in mind, we chose the iron(II) complexes of octaethylporphyrin and tetraphenylporphyrin, (OEP·Fe(II))py₂ and (TPP·Fe(II))py₂, respectively, as models of the heme and benzene as the hydrophobic environment surrounding the heme.

Skatole (2 mmol) in benzene (10 ml) is difficult to react with oxygen (1 atmosphere) at room temperature (23°±2°C). However, in the presence of TPP·Fe(II)py₂ or OEP·Fe(II)py₂ (20 μmol, substrate/TPO model molar ratio: 100/1) oxygen absorption easily occurs and skatole is converted to 2-formamidoacetophenone (FA) as shown in Reaction 2.



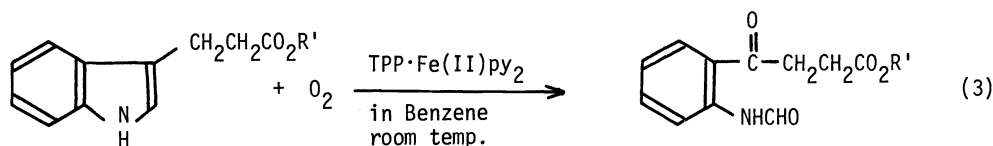
The oxygenation was carried out by oxygen gas (1 atm.)/benzene solution contact method. In this condition the mole ratio of skatole to dissolved oxygen in benzene is 37:1. Such a high [substrate]/[O₂] ratio is important to simulate the oxygenase reaction. This reaction was monitored by the measurement of oxygen absorption and GLC of the reaction mixture. The relationship between skatole conversion and reaction time is shown in Fig. 5. The conversion of skatole increases with time (Fig. 3). At less than 40~50% conversion, FA is the sole product. On the other hand, at over 50% conversion, products other than FA are formed and the amount of byproducts formed increases with time. For example, at 90% conversion of skatole, the yield of FA is 44% and the remainder (56%) of the skatole becomes 2-aminoacetophenone and polymeric materials. Both porphyrins (TPP·Fe(II)·py₂ and OEP·Fe(II)·py₂) show almost the same catalytic activity for this reaction. When N-ethylimidazole is added to this reaction system, the reaction of skatole with oxygen is depressed with the amount of N-ethylimidazole added (Fig. 5). This is ascribed to the masking effect of the active coordination site by the stronger ligand, indicating the importance of the coordination of skatole to Fe(II) porphyrin. The spectroscopic monitoring of the reaction mixture indicates that the μ-oxodimer (TPP·Fe(III)OFe(III)·TPP) is slowly formed by the oxidation of TPP·Fe(II) complex. However it was found that (1) the catalytic activity of the μ-oxo dimer for this oxygenation is very low compared to that of TPP·Fe(II)py₂, and (2) the μ-oxo dimer

and TPP·Fe(III)X are almost inactive catalysts for the oxygenation of 3-t-butyl indole, which is easily oxygenated by TPP·Fe(II)py₂ to form the same type product as FA. Although oxygen coordinates to the Fe(II) of iron-porphyrin in aprotic solvents, the electronic and NMR spectra of the skatole-Fe(II)TPP and skatole-Fe(III)TPP systems indicate that σ coordination of skatole NH toward iron is difficult to accomplish. Therefore, the π interaction of skatole with the iron of Fe(II)TPP·O₂ and the σ-coordination of skatole N⁻ (produced through deprotonation by iron porphyrin) with the iron of Fe(II)·TPP complex should occur for the skatole → FA reaction; the equilibrium concentration of this complex should be small. When 2,3-dimethylindole, which is a stronger electron donor than skatole is used instead of skatole, the more rapid oxygenation reaction (Fig. 5) occurs, producing 2-acetamidoacetophenone. Although tryptophan does not dissolve in benzene, 3-indolepropionic acid ester (R[']=CH₃~C₆H₁₃) is soluble in benzene, and converts smoothly to the corresponding 2'-formamidophenyl-4-ketopropionic ester (see Reaction 3). The reaction proceeds more effectively with increasing alkyl chain length (R[']). Therefore, judging from the oxygenation activity, the high product selectivity, the high product yield, and the structural similarity to TPO active site, the iron(II)porphyrin system is considered to be the best model of TPO active site. As for the substrate specificity of iron(II)porphyrin catalyzed oxygenation, 3-alkyl and 2,3-dialkylindoles undergo the TPO type reaction. However, indole, 2-methylindole, 1,2-dimethylindole, and 1,3-dimethylindole do not react with oxygen under the above conditions. For indole derivatives to be oxygenated catalytically by Fe(II)porphyrin (heme), they must have a 3-alkyl group and a N-H group. This substrate specificity is different than those in photosensitized oxygenation by singlet oxygen (Ref. 17~19) and radical autoxidation of indole derivatives (Ref.20), suggesting that the active oxygen species produced from 3-alkylindole-Fe(II)porphyrin-O₂ system is different than the singlet

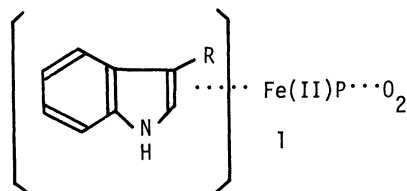


1. 2,3-dimethylindole
2. Skatole
3. Skatole (Skatole: N-ethylimidazole=1:0.23)
4. Skatole (Skatole: N-ethylimidazole=1:5.5)

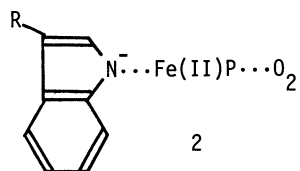
Fig. 5 Oxygenation reaction of 3-alkylindoles



oxygen and radical oxygen species from autoxidation. Superoxide ion ($\cdot\text{O}_2^-$) might be produced as the active oxygen from the Fe(II)porphyrin and molecular oxygen system (binary system). However, superoxide (18-crown 6 complexed KO₂) in benzene does not react with skatole under the above reaction condition. If this reaction occurs to give FA, the reaction is stoichiometric and not catalytic. The substrate specificity mentioned above also excludes the possibility of oxygen activation via the π coordinated skatole Fe(II)-porphyrin-O₂ complex (1).



So the oxygen activation in this reaction system seems to occur via a skatole anion-coordinated Fe(II)porphyrin- O_2 complex (2).

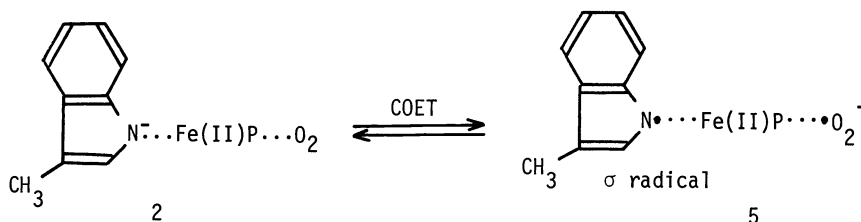


2.2 Oxygen activation mechanism

To gain insight into the oxygen activation mechanism of this model system ESR investigation of the following systems carried out in toluene: 1. TPP·Fe(II)·py₂ (10 μmol)-skatole (1 mmol); 2. TPP·Fe(II)py₂-skatole-air; 3. TPP·Fe(III)·OAc-skatole; and 4. Skatole-air system. Using air instead of oxygen, we can control the reaction rate to get the ESR spectra for Systems 1-4 at different times. The ESR measurement was carried out at -196°C (liq. N₂ temperature) after allowing the solution to stand at 23°C±2° for a given period of time. For systems 1,3, and 4 no ESR signal was detected for one day immediately after preparation. In the absence of molecular oxygen electron transfer does not occur between skatole (or skatole anion) and the Fe(III)porphyrin. Immediately upon contact with air, the high spin complex ($g \sim 6.1$) due to Fe(III)TPP·py (pentacoordinated complex) is observed together with the free radicals whose g values are 1.99 - 2.04 and the low spin Fe(III) complex. The formation of a pair of low spin complexes due to the hexacoordinated Fe(III)-TPP complexes ($g=2.66, 2.19, 1.80$ and $g=2.31, 1.93$) occurs with time. Of those, one should be the Fe(III)TPP·py₂ and another the product-coordinated Fe(III)TPP complex. The appearance of ESR absorptions due to Fe(III) complexes (high and low spin) indicates that a part of Fe(II)TPP complex is converted to the Fe(III) state by reaction with molecular oxygen. Absorptions other than those assigned to the Fe(III) complex are observed. The absorption at $g=1.99$ is assigned to the superoxide ion ($\cdot O_2^-$) (Ref. 21). There is a very broad band centered at $g=2.04$ that has hyperfine splittings. The each hyperfine constant is very large (ca. 20G) compared with those for the pyrrole π radicals (4) (Ref. 22); a large hyperfine constant is characteristic of the σ radical. Therefore, this radical can be identified as the following skatole σ radical (3).



Other than $\cdot O_2^-$ and the skatole σ radical (3), a radical exists having a g -value of 2.002 with unclear hyperfine splitting. This radical may be the π radical (4) from the skatole anion. The σ radical (3) and superoxide ion ($\cdot O_2^-$) are considered to be formed by electron transfer from the skatole anion to oxygen in the ternary complex (2), which is composed of strong electron donor and weak electron acceptor through Fe(II)porphyrin. In such a complex (D...Fe(II)P...A type complex, D: electron donor, A: acceptor), electron transfer from the donor to the acceptor should occur more easily than the direct electron transfer in the D...A complex, because in the former the cooperative interaction of the three components should decrease the energy barrier of the electron transfer.



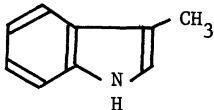
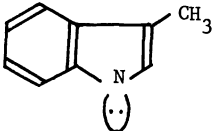
The observed ESR spectra strongly support the interpretation that no electron transfer occurs between a skatole anion and Fe(III)P in the binary system in toluene (hydrophobic media) at room temperature. On the other hand, under same conditions electron transfer from skatole anion to oxygen occurs in the ternary complex (2). This is an activation mechanism of

molecular oxygen in the iron(II)porphyrin catalyzed oxygenation of skatole. We have termed this type of electron transfer the cooperative (or concerted) electron transfer (COET).



When the electron accepting power (electron affinity) of the acceptor is less than that of molecular oxygen (EA: 0.43 eV), the electron donating power (ionization potential) of the donor must be larger than that of skatole anion for COET to occur. The MINDO/3 ionization potentials (I_p) for skatole and the skatole anion are shown in Table 4. This table indicates that by the deprotonation of the skatole NH, the HOMO (π) ionization potential becomes

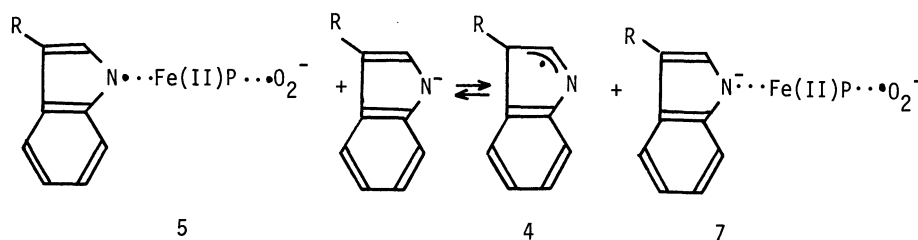
Table 4 MINDO/3 Ionization Potential for Skatole and Skatole Anion

Species	Ionization Potential (eV)		
	HOMO (π)	7.665	7.63 (obs [*])
	HOMO (π)	2.291	
	N-lone pair	3.101	

* H. Gusten et al., Z. Naturforsch., 319, 1051 (1976).

significantly smaller (7.665 eV \rightarrow 2.291 eV). Also, the N-lone pair ionization potential (3.101 eV) of the skatole anion is close to the HOMO (π) ionization potential (2.291 eV). Therefore, the skatole anion is considered to be strong electron donor. From the ionization potentials of HOMO (π) and N-lone pair in non-interacted states, the generation of the π radical of the skatole anion should be easier than the generation of the σ radical (3). The observed exclusive formation of σ radical (3) in the ternary system might be caused by the effect of coordination with the iron(II) of the heme. The planar ligand, porphyrin, should make the axial coordination of both the donor and the acceptor possible and should also be useful in the stabilization of this system.

From the arguments mentioned above, the iron(II)porphyrin catalyzed oxygenation of skatole (and related compounds) most likely proceeds as shown in Scheme 1, which involves the π radical (4) intermediate. Process 1 is the equilibrium formation of the skatole anion-coordinated iron(II)porphyrin (6), which occurs with Fe(II) and solvent (B, π base) assistance. When the electron relay system 2 is formed by oxygen coordination, very rapid COET should take place to give the coordinated skatole σ radical and superoxide ion. Judging from the HOMO (π) and N-lone pair levels, this σ radical can interact with skatole anion to give the π radical (4).



This π radical (4) should react easily with the superoxide ion of 7 to give the final product 8 via the most probable endo peroxide intermediate. The reproduced skatole anion-coordinated Fe(II)porphyrin (6) by process 3 is again reacted in Process 2. The iron(II)porphyrin catalyzed oxygenation of skatole should proceed in this manner. This mechanism could be applicable to the TPO reaction shown in Scheme 2, taking into account the characteristics of the TPO reaction and Fig. 4. In Scheme 2, SH represents L-tryptophan and 9 represents

TPO. First, the SH is incorporated into the activity control site to form 10 (corresponding to 6); a second incorporation of SH should occur at the binding site (recognition). The TPO reaction should proceed by the subsequent reactions (11→12→13→14→10) and repetitions of these reactions.

In order to get spectroscopic evidence for COET, we have examined the electron transfer from RS^- (strong donor) to carbonyl (weak acceptor, $EA_{CO} -1.75$ eV, cf, $EA_{O_2} 0.43$ eV, $EA_{I_2} 2.6$ eV) in the stable $RS^-\cdots Fe(II)OEP\cdots CO$ complex instead of in the extremely unstable $RS^-\cdots Fe(II)OEP\cdots O_2$ complex (Ref. 23). The observed carbonyl stretching vibrations of $Fe(II)OEP\cdots CO\cdots L$ are shown in Table 5. From this table, it is evident that alkanethiolate

Table 5 Carbonyl Stretching Vibrations in Stable Metallo Porphyrin Complexes

Complex	Solvent	L	ν_{CO} (cm^{-1})
$Fe(II)OEP\cdots CO\cdots L$	Benzene	none	1975
$Fe(II)OEP\cdots CO\cdots L$	Benzene	$\bar{S}R$	1950
$Fe(II)OEP\cdots CO\cdots L$	DMF	none	1948
$Fe(II)OEP\cdots CO\cdots L$	DMF	$\bar{S}R$	1923

anion reduces the wave number of the carbonyl stretching by 25 cm^{-1} for the $Fe(II)$ complex, which clearly indicates COET charge transfer. The COET process in $L\cdots Fe(II)P\cdots O_2$ complex will be predicted by the ionization potential of the axial ligand L, although we have not yet the distinct criterion for ionization potential value. If the ionization potential of L is larger than ca. 8 eV, the cooperative one electron transfer would not be expected to occur. Such examples of L are pyridine (I_p , 9.66 eV for N lone pair, 9.80 eV (π)), imidazole (I_p , 9.76 eV for N lone pair), N-methylimidazole (I_p , 9.63 eV for N lone pair) and CH_3SH (9.44 eV for S lone pair). The strong coordination of imidazole is useful to stabilize the oxygen adduct. On the other hand, if the ionization potential of L is smaller than ca 4 eV, the cooperative one electron transfer should be expected to occur. Such examples of L are CH_3S^- (I_p , 1.92 eV), and CH_3O^- (I_p , 2.3 eV) other than \bar{N}^- such as 3-alkylindole anion. Oxygen activation in cytochrome P-450 and action mechanism of bleomycin, an anticancer agent, can also be explained by the COET concept.

Acknowledgement

I would like to express my appreciation to the following collaborators who have contributed to the work described above: Prof. H. Ogoshi, Dr. S. Yoneda, Dr. H. Sugimoto, S. Mitachi, K. Kawabe, Dr. K. Imai and Prof. I. Tyuma. I wish also to thank the ministry of Education, Science and Culture, Japan for financial support.

REFERENCES

1. M. F. Perutz, *Brit. Med. Bull.*, **32**, (3) 193 (1976); *Nature* **228** 726 (1970).
2. H. Watari, H. Ogoshi, I. Iizuka, *Chemistry of Hemoproteins*, Kagakudojin, Kyoto (1978).
3. E. Antonini, M. Brunori, *Hemoglobin and Myoglobin in Their Reactions with Ligands*, Elsevier, New York, (1971).
4. J. P. Collman, *Acc. Chem. Res.*, **10**, 265 (1977).
5. H. Ogoshi, K. Kawabe, S. Mitachi, Z. Yoshida, K. Imai, I. Tyuma, *Biochim. Biophys. Acta* **581**, 266 (1979).
6. K. Kawabe, Z. Yoshida, K. Imai, I. Tyuma, H. Ogoshi, to be published.
7. K. Imai, H. Morimoto, M. Kotani, H. Watari, W. Hirota, M. Kuroda, *Biochim. Biophys. Acta*, **200**, 189 (1970).
8. T. Takano, *J. Mol. Biol.*, **110**, 537, 569 (1977).
9. H. Sugimoto, *Ph.D. Thesis* (Kyoto University, 1979).
10. O. Hayaishi, *Oxygenase*, Academic Press, New York, (1962).
11. H. S. Mason, *Ann. Rev. Biochem.*, **34**, 595 (1965).
12. O. Hayaishi, *Ann. Rev. Biochem.*, **38**, 21 (1969).
13. O. Hayaishi, M. Nozaki, *Oxygenase*, Tokyo Univ. Press, Tokyo (1973).
14. O. Hayaishi, *Molecular Mechanisms of Oxygen Activation*, Academic Press, New York (1974).
15. Y. Ishimura, M. Nozaki, O. Hayaishi, M. Tamura, I. Yamazaki, *J. Biol. Chem.*, **242**, 2574 (1967).
16. K. O. Hardmann, E. H. Eylor, F. R. Gurd., *J. Biol. Chem.*, **241**, 432 (1966).

17. N. A. Evans, Aust. J. Chem. 24, 1971 (1971).
18. I. Saito, M. Imuta, T. Matsuura, Chem. Lett., 1972, 1173, Synthesis, 1976, 255.
19. I. Saito, T. Matsuura, M. Nakagawa, T. Hino, Acc. Chem. Res., 10, 346 (1977).
20. R. J. Sundberg, The Chemistry of Indoles, Academic Press, New York (1970).
21. M. E. Peover, B. S. White, Electrochim. Acta, 11, 1061 (1966).
22. A. Samuni, P. Neta, J. Phys. Chem., 77, 1629 (1973).
23. H. Ogoshi, H. Sugimoto, Z. Yoshida, Bull. Chem. Soc. Jap., 51, 2369 (1978).